https://doi.org/10.5194/egusphere-2024-1807
Preprint. Discussion started: 15 July 2024

Assessment of Continuous Flow Analysis (CFA) for High-Precision Profiles of Water Isotopes in Snow Cores

Remi Dallmayr[1], Hannah Meyer[2], Vasileios Gkinis[3], Thomas Laepple[5,6], Melanie Behrens[1], Frank Wilhelms[1,4] and Maria Hörhold[1]

[1]Alfred-Wegener-Institut Helmholtz-Zentrum für Polar-und Meeresforschung, Bremerhaven, Am Handelshafen 12, 27570 Bremerhaven, Germany
[2]Institute of Meteorology and Climate Research (IMK-TRO), Department Troposphere Research, Karlsruhe Institute of Technology (KIT), PO 3640, 76021 Karlsruhe, Germany
[3]Niels Bohr Institute Physics of Ice, Climate and Earth, Tagensvej 16, 2200 Copenhagen, Denmark
[4]GZG Abt. Kristallographie, University of Göttingen, Göttingen, Germany
[5]Alfred-Wegener-Institut Helmholtz-Zentrum für Polar-und Meeresforschung, Potsdam, Telegrafenberg A45, 14473 Potsdam, Germany
[6]University of Bremen, MARUM – Center for Marine Environmental Sciences and Faculty of Geosciences, 28334 Bremen, Germany

Correspondence to: Remi Dallmayr (remi.dallmayr@awi.de)

Abstract. An efficient measurement of stable water isotopes in snow profiles is required to improve our understanding of the climate signal preserved in polar firn and ice and to improve the signal to noise ratio in climate reconstructions from ice cores. To allow the analysis of snow cores, we modified a Continuous Flow Analysis system at AWI to analyze multiple snow-cores in a reasonable time and with high-quality. We here describe the CFA-setup and isotope measurements, including the methodology to quantify the mixing of the isotope signal induced by the system along its different steps, leading to smoothing of the final isotopic signal. With our obtained mixing lengths for the instrumental setup and the continuous analyze of snow-cores of 14 and 30 mm, respectively, we show that with such highly porous cores the main mixing occurs through percolation. Based on these findings we suggest technical improvements to match the imposed analytical challenge and fully resolve the stable water isotope variations from low-accumulation snow-cores. Finally, comparing discrete and CFA based profiles, we illustrate that diffusion within the snow-cores takes place during storage time in cold facilities, underlining the need of near-time analysis of collected snow cores using for example Snow-CFA systems.

1 Introduction

Stable water stable isotopes ($\delta^{18}O$ and δD) in polar ice cores are commonly used to derive paleo-temperatures (Jouzel et al., 1997). In low accumulation areas of the East Antarctic ice sheet, the reconstruction of past climates over large time scales, i.e. several interglacial periods are possible (e.g., Petit et al., 1999; Kawamura et al., 2017), while at the same time the reconstructions of shorter time scales, i.e. interannual-to decadal climate variabilities, is highly problematic (Ekaykin et al., 2002; Hoshina et al., 2014; Münch and Laepple, 2018). The reason lies in the large stratigraphic noise (Fisher et al., 1985) imposed by (post-) depositional processes such as wind-redistribution, adding non-climatic variability to the local climate

https://doi.org/10.5194/egusphere-2024-1807
Preprint. Discussion started: 15 July 2024

record. In fact, ice core records from most areas on the East Antarctic Plateau are dominated by noise (Laepple et al., 2018, Casado et al.,2020). However, recent studies (Münch et al. 2016, 2017) showed that averaging over a large number of independent vertical profiles allows for inferring a common local climate signal from the stacked stable water isotope record. These findings imply, that it needs a high number of high-resolution snow profiles at an ice core drill site in order to quantify the noise. Commonly, snow profiles were sampled manually at a snow pit trench wall or recently by a snow liner technique (Schaller et al., 2016), where snow cores are extracted from the snow pack and are cut manually into discrete samples. However, by increasing the number of necessary snow cores for each site, the work load for the analysis of discrete samples for their isotopic composition is increasing beyond a feasible manner.

To this end the previously applied Continuous Flow Analysis (hereafter CFA) for ice cores can serve as a solution, as ice cores do not have to be cut prior to analysis, but can be melt and analyzed in one piece. By continuously melting a longitudinal section of a core sample on a chemically inert Melt-Head (hereafter MH), the CFA provides high-resolution measurements of stable water isotopes at high-pace (Gkinis et al., 2011; Dallmayr et al., 2016; Jones et al., 2017) in parallel with other proxies such as concentrations of chemical impurities (Osterberg et al., 2006; Bigler et al., 2011). However, such system is commonly not used with shallow firn and snow cores due to the percolation occurring during the melting within the highly porous samples. A first approach to apply CFA to snow-cores is the LISA Box (Kjaer et al., 2021) for measurements in the field, where a snow core of 10 cm-diameter and 1 m-length is melted on a specifically developed MH. Here the meltwater is analyzed for conductivity and peroxide, allowing a quick estimation of age and accumulation rate with high quality. But due to its application in the field, measurements of other parameters such as stable water isotopes are not possible with this set-up.

In order to be able to measure stable water isotopes in snow cores by CFA, we modified the CFA-system developed at the Alfred-Wegener-Institut, Helmholtz-Zentrum für Polar- und Meeresforschung (hereafter AWI) using the MH proposed by Kjaer et al. (2021). We developed a method to characterize on a routine base the mixing of the system by (1) means of isotopic standards, and (2) comparison to discrete measurements. Doing so, we were able to separate and quantify the contribution of different components of the CFA to the overall mixing of the signal, with the percolation in the snow just above the MH to be the major contributor.

2. Material and method

2.1. Experimental set-up

The system to analyze 1-meter snow-cores consists of a melting unit, a degassing unit, an electrical conductivity unit, a water isotope measurement unit, a micro-particles detection unit, a fraction collector module, and a datasets synchronization system (Fig. 1). The MH is constructed such, that it separates the potentially contaminated outer part of the snow core from the clean inner part. The melt water of the outer part of the snow core is drained to an extra collection unit for non-sensitive measurement, while the melt water of the inner part is driven to a degassing unit (debubbler, hereafter DB) by a peristaltic pump (Ismatec IPC) through a perfluoroalkoxy (PFA) tubing with 1/16” outer diameter (OD) and 0.76 mm inner diameter (ID). Downstream

https://doi.org/10.5194/egusphere-2024-1807
Preprint. Discussion started: 15 July 2024

of the DB, a second peristaltic pump (Ismatec IPC) drives the now bubble-free water stream to a polyether ketone (PEEK) manifold (P-150, Idex), from where sub-streams are distributed to the different analytical units through PFA tubing (0.51 mm ID). During periods where no sample is melted, the analytical units are fed with ultrapure water (Millipore Advantage, Milli-Q ≥ 18.2 MΩ.cm-1, hereafter MQ).

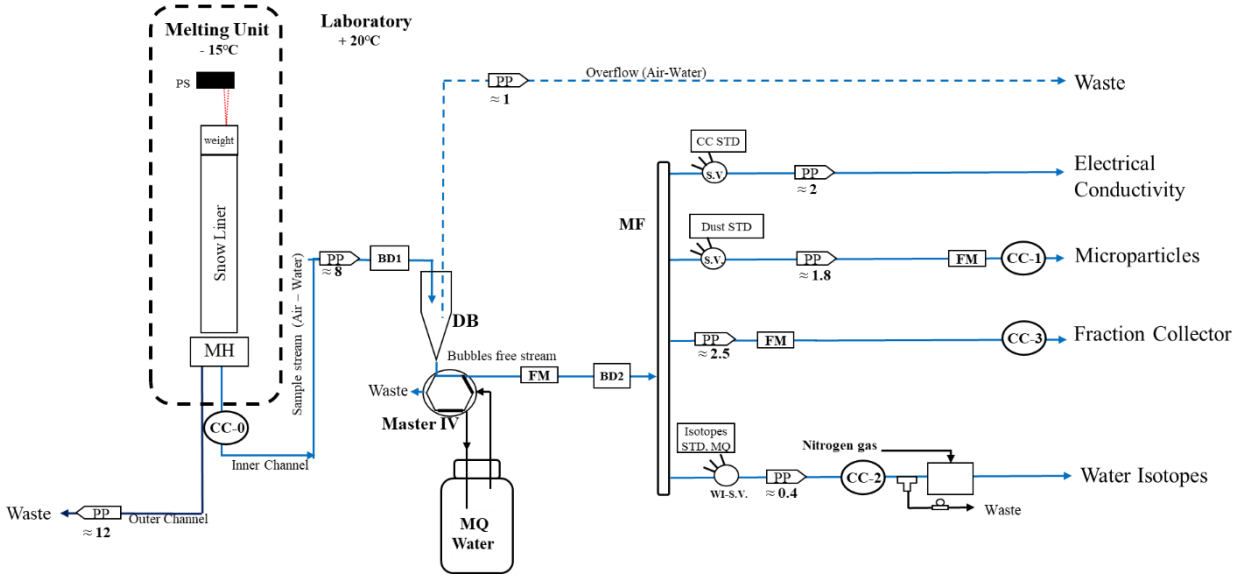

Figure 1: Setup of the AWI-CFA system to measure snow cores. The snow-core is held in a snow sample holder (SSH) and melted on a Melt-Head (MH) in a -15°C environment (left hand side). The laser positioning sensor (PS) determines the distance to the weight (W) placed on the top of the core. In the laboratory, the conductivity detectors for synchronization (CC-i); an injection valve (Master IV) switching between MQ water and ice sample; a degassing unit (DB); a manifold (MF); selection valves (SV) for analytical units switching between MQ, sample, and standards. All analytical measurements are indicated. Liquid flow sensors (FM) monitor the flow behaviour of the system. Finally, detection of air bubbles takes place upstream (BD1) and downstream (BD2) of the DB. All indicated flow values are expressed in ml min-1.

Snow core Melting unit

The melting unit features a 10 cm inner diameter and 120 cm long tube made of acrylic and positioned centrally above the MH (Fig. 2a), guiding the sample during the experiment. A light weight (~150 g) is placed atop of the snow core to stabilize the melt-flow, and is covered on both sides with a 1 mm thickness layer of PTFE to prevent contamination. Following the work of Dallmayr et al. (2016), a high-accuracy laser positioning senor (Way-con, LLD-150-RS232-50-H) determines the distance from the sensor and the top of the weight with a precision of 0.1 mm in order to derive accurate melt-speeds and to assign precise depths to the datasets generated.

https://doi.org/10.5194/egusphere-2024-1807
Preprint. Discussion started: 15 July 2024

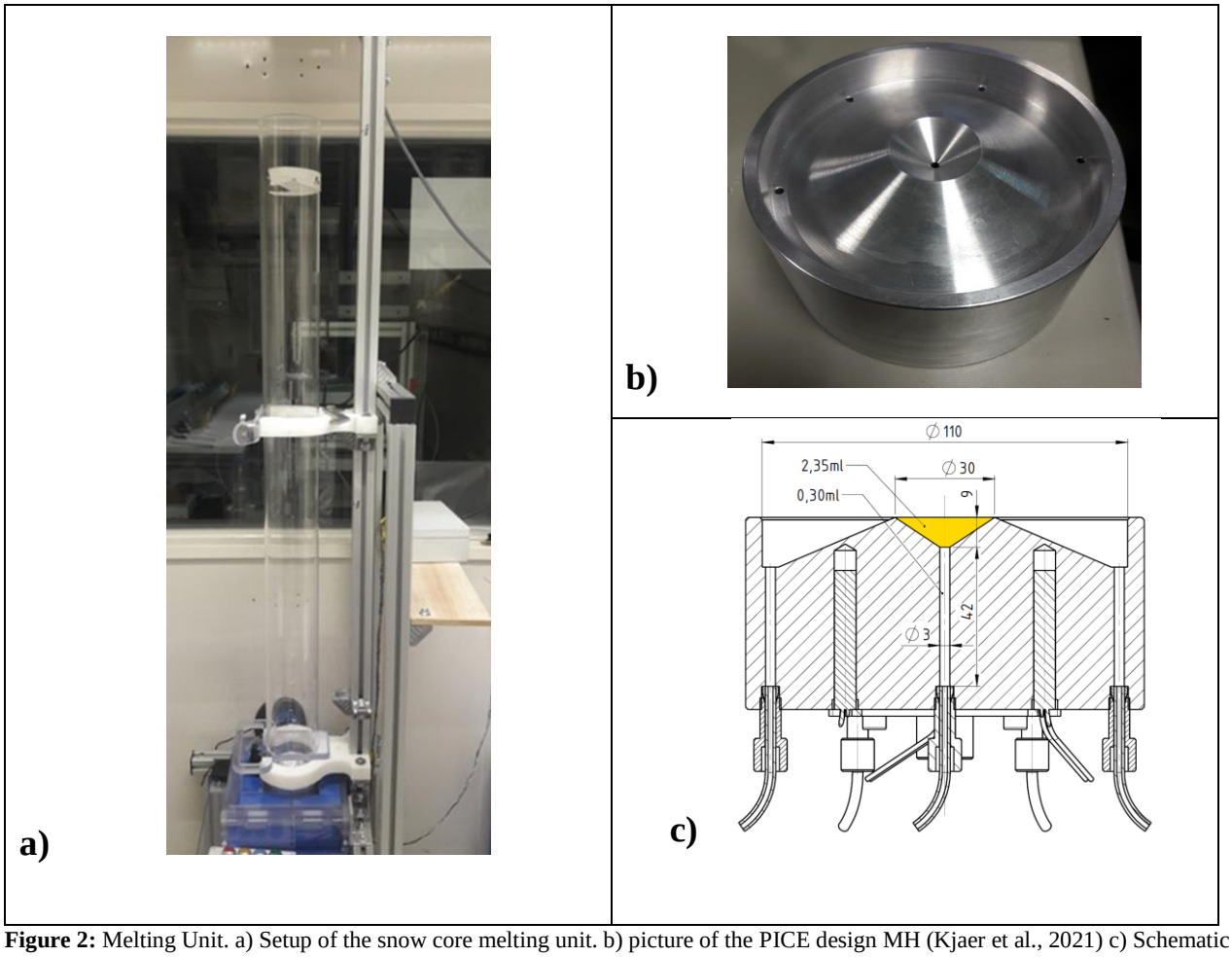

Figure 2: Melting Unit. a) Setup of the snow core melting unit. b) picture of the PICE design MH (Kjaer et al., 2021) c) Schematic view of the MH, showing the dimension of the inner-channel concave volume (orange).

The MH for snow-cores (Fig. 2b) is based on the Physics of Ice, Climate and Earth, (Copenhagen, Denmark, hereafter PICE) design used by Kjaer et al. (2021), made of aluminum, and manufactured at the AWI in Bremerhaven, Germany. Through a concave volume at the inner-channel (highlighted in Fig. 2c), the shape of the MH prevents mixing of clean inner-part with the potentially contaminated outer-part of the core sample. The temperature of the MH is regulated by a Proportional-Integrated-Derivative (PID) temperature controller (JUMO corporate, Germany) attached to eight 125 W heating cartridges and a conventional thermocouple type J.

https://doi.org/10.5194/egusphere-2024-1807
Preprint. Discussion started: 15 July 2024

Debubbling Unit

As air in the sample stream leads to significant effects and interferences in the liquid detectors, a separation of air and liquid via a debubbling unit (hereafter debubbler, DB in Fig. 1) is required. The incoming flow drips into a micropipette opened to the air, releasing the air bubbles to the atmosphere by buoyancy and leading to a bubble-free flow downstream. Furthermore, regarding the inhomogeneous distribution of air bubbles in the incoming flow, and unpredictable stops of the core melt, maintaining an amount of water in the debubbler (safety volume) is essential. To that aim, an overflow-tube (Fig. 1) connected to a peristaltic pump is continuously sucking air, or an overflow if the water-level within the pipette gets in contact. We set the height of this overflow-tube to a minimal safety volume of ~1 ml. A bubble detector located upstream of the unit (Fig. 1) monitors the variability of air in the incoming stream. A second bubble detector is located downstream of the unit (Fig. 1), monitoring, warning and recording the detection of air.

Analytical measurements

The CFA-system performs the online measurement of electrical conductivity (conductivity-cell model 3082, Amber Sciences Inc., USA, Breton et al., 2012) and micro-particles counting and sizing (Abakus, Klotz GmbH, Germany, Ruth et al., 2002). Stable water isotopes ($\delta^{18}O$ and δD) mixing ratios are continuously measured by a Cavity Ring Down Spectrometer (CRDS, Picarro Inc, USA, Maselli et al., 2013). To obtain the continuity and stability of a micro-flow rate of vapor as required by the instrument, a stream vaporization module was made based on the original method of Gkinis et al. (2010). A micro-volume tee is used to split a micro-flow into a 50 µm ID fused-silica capillary from the incoming stream. The waste line featuring a smaller ID, a back-pressure is enabled and pushes the micro-flow through the capillary towards the oven where mixing with dry air occurs before injection to the instrument. To control the back-pressure precisely and efficiently, we divided the waste line using a second tee and added to one sub-waste line a 10-turn micro-metering needle valve (Dallmayr et al., 2016). Schematic and technical details of the water isotope line are provided in Appendix A.

In addition to the online measurements, fractions are carefully collected under a laminar flow bench for further offline measurements of chemical impurities by Ion Chromatography (normative precision of <10%, Göktas et al., 2002).

Additional electrical conductivity measurements are performed at the melting unit outlet (CC0 in Figure 1, Amber Sciences model 1056, USA) as well as near the inlet of each detection unit (CC1 to 3 in Fig. 1, contactless conductivity measurement, Edaq, Australia). Such duplicated measurements allow for a straightforward and efficient synchronization of the different datasets during data processing (Dallmayr et al., 2016).

Control and data acquisition, processing system, analysis of diffusion

All devices are connected to the controlling computer, using a software developed with LabVIEW 2012. Drivers are either provided by manufacturers (pumps, flowmeters) or developed to suit the purpose (Laser positioning, actuated valves, bubbles detectors, all analytical units). Analytical data are recorded every second, and are processed after the experiment by using a

https://doi.org/10.5194/egusphere-2024-1807
Preprint. Discussion started: 15 July 2024

second piece of software also developed with LabVIEW 2012. The analyzes of isotopic diffusion are realized using algorithms developed with the software R (R Core Team, 2018).

2.2. Characterization of mixing

CFA-systems are known to diffuse, mix and attenuate the original isotope signal (Gkinis et al., 2011; Jones et al., 2017). The resulting smoothing of the original signal can be described as a mathematical convolution:

$$\delta_m(t) = [\delta_0 \circledast G](t) = \int \delta_0(\tau) G(t-\tau) d\tau \quad (1)$$

With δ_m the measured value and δ_0 the original (isotopic) value of the sample at time *t*. G is a smoothing filter denoting the impulse response of the system and $\circledast$ refers to the convolution operation.

We here address the characterization of this mixing by analyzing the impulse response of the system, i.e. we analyze the derivative of the response of the system to an instantaneous isotopic change. Previously two approaches have been proposed to treat the step response:

First, Gkinis et al. (2011) fit this so-called step response of the system to a scaled cumulative distribution function (hereafter CDF) of a normal distribution, as:

$$\delta_{normal}(t) = \frac{A}{2}\left[1 + erf\left(\frac{t-t_0}{\sigma\sqrt{2}}\right)\right] + B \quad (2)$$

with A and B the isotopic values of the step scaled, t_0 the initial time, and σ the standard deviation. All parameters are determined by means of least square optimization. In the case of a normal distribution, the impulse response of the CFA-system is described by a Gaussian impulse probability density function (PDF):

$$G_{normal}(t) = \frac{1}{\sigma_{normal}\sqrt{2\pi}} e^{-\frac{(t-t_0)^2}{2\sigma_{normal}^2}} \quad (3)$$

Here, the standard deviation of the Gaussian PDF (σ_{normal}) characterizes the mixing length of the system, expressed in seconds. Later, these values can be converted into a mixing length expressed in mm by applying the measured melt-speed.

Second, because of the skewed shape of the impulse response, Jones at al. (2017) proposed an implementation from normal CDF to two multiplied lognormal CDFs ($\delta_{log-log}(t) = \frac{C}{2}\left[1 + erf\left(\frac{t-t_1}{\sigma_1 * \sqrt{2}}\right)\right]\left[1 + erf\left(\frac{t-t_2}{\sigma_2\sqrt{2}}\right)\right] + D$). This approach provides a slightly better fit to the signal, but the diffusion length is then retrieved using an additional function fitting the two lognormal CDFs. The derived mixing length requires thus a careful interpretation due to these additional uncertainties.

We apply both approaches, compare the results and assess the contribution of the different CFA units to the overall mixing length using the Gaussian distribution.

2.3 Snow-core samples

To evaluate the performances of the CFA-system, we compare continuous analysis with discrete samples via six 1-meter long snow-cores (KF13 to KF18). The snow cores originate from Kohnen station (0°04E 75°00 S, 2892 m.a.s.l.), Dronning Maud

https://doi.org/10.5194/egusphere-2024-1807
Preprint. Discussion started: 15 July 2024

Land (Oerter et al., 2009). This area is characterized by an accumulation rate of 75 mm w.e. yr^{-1} over the last 50 years (Moser et al., 2020). The snow cores were taken following the procedure by Schaller et al, (2016) from a trench excavated during the 2014/2015 season (Münch et al., 2017), where the cores used in this study correspond to an absolute snow depth of 240-340 cm, with a horizontal distance of 5 m.

From all snow cores a calotte of 25 mm thickness lengthwise was cut into discrete samples at 22 mm resolution. The discrete samples were analyzed at AWI Potsdam in 2015 (hereafter dataset discrete-15). In 2019, a second discrete dataset was obtained with a similar 22 mm depth-resolution, just prior to the continuous analysis of the remaining core (55 mm wide). For this second discrete dataset (hereafter discrete-19), four cores (KF13-16) were analyzed for isotopic composition whereas the remaining two cores (KF17 and 18) were analyzed for ion chromatography at AWI Bremerhaven. For the discrete datasets 2015 and 2019, single isotopic measurements are provided with an accuracy of 0.1 ‰ for $\delta^{18}O$, and 1.5 ‰ for δD.

3. Results – Stable Water Isotopes

3.1 Instrumental behavior

The behavior of the CRDS is determined by Allan variance test (Allan, 1966) over a period longer than 12 hours by continuous injection of MQ water. Such a test allows the investigation of the noise and drift of our spectrometer with respect to the integration time.

The Allan variance is defined as:

$$A_{var} = \frac{1}{2(n-1)} \sum_{i=1}^{n-1} (y(\tau)_{i+1} - y(\tau)_i)^2 \quad (4)$$

with y(τ) the average value of the measurements during an integration interval of length τ, and n being the total number of intervals. The results show the linear decrease of the Allan deviation (square root of Allan variance) up to an optimal deviation for an integration time of ~6000 s (Fig.3). Instrumental drift starts slightly earlier than 104 s with low deviation (0.01 ‰ for $\delta^{18}O$ and 0.1 ‰ for δD) up to $4*10^4$ s. Therefore, for our snow-cores study and the longest single analysis segment of <3000 s, a single calibration per core is necessary.

https://doi.org/10.5194/egusphere-2024-1807
Preprint. Discussion started: 15 July 2024

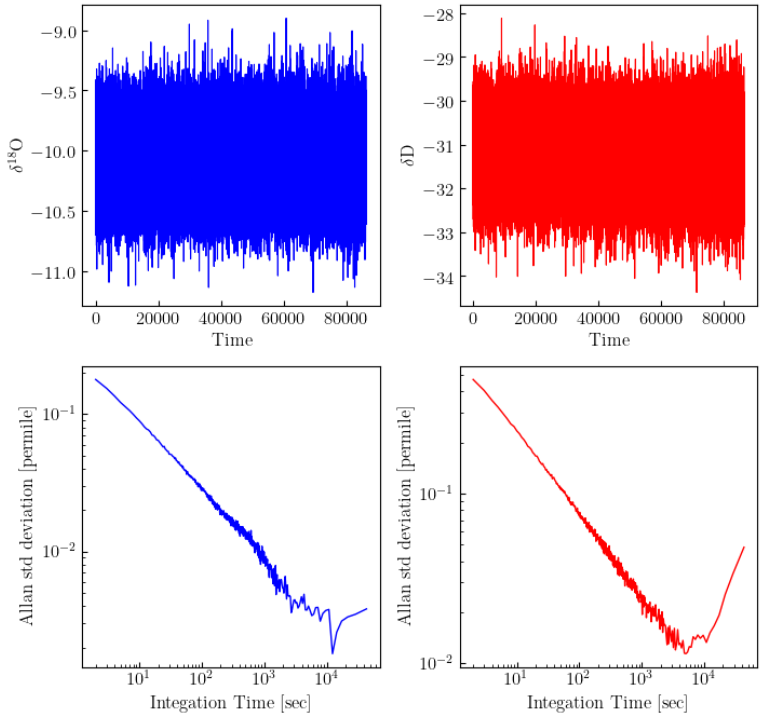

Figure 3: >12 h of Allan deviation analysis for $\delta^{18}O$ (left panel, in blue), and δD (right panel, in red).

190

3.2 Calibration to the VSMOW-VSLAP scale, precision of continuous dataset

Calibrations of the raw data are performed using 3 laboratory-standards (Table 1) which are annually calibrated to the international VSMOW-VSLAP scale. The last 2 minutes of each >15 min laboratory-standard run is averaged. Based on the measured and real values of the standards, a linear regression fitting the 3-point is applied and defines the calibration
195 coefficients (Fig. 4).

	NZE	TD1	JASE
$\delta^{18}O$	-19.85	-33.85	-50.22
δD	-152.7	-266.2	-392.5

Table 1: Isotopic composition of the laboratory standards used for VSMOW calibrations, in ‰.

https://doi.org/10.5194/egusphere-2024-1807
Preprint. Discussion started: 15 July 2024

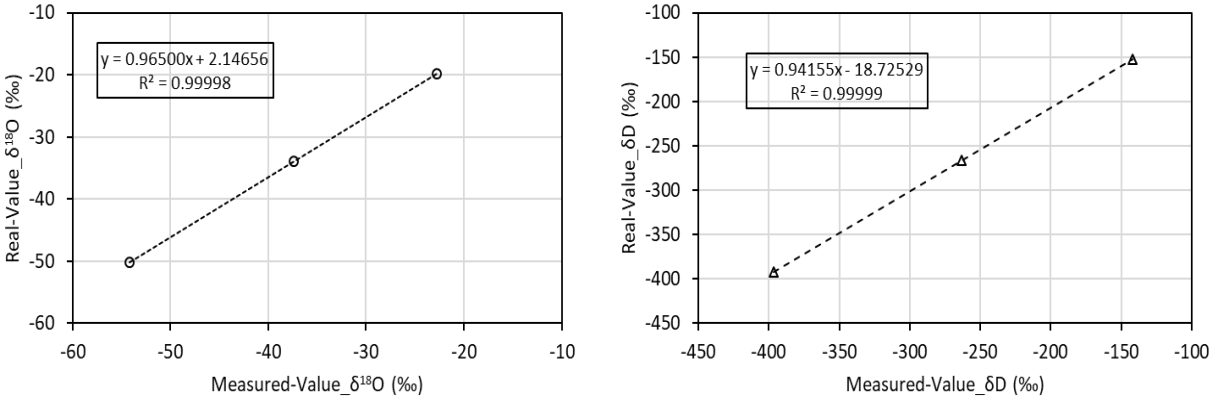

Figure 4: VSMOW three-points calibration with laboratory standards NZE, TD1, JASE (left: $\delta^{18}O$, right: δD).

In addition to the calibration, the laboratory-standards are used to infer the precision of our measurements, defined as the level of internal agreement among independent measures. The standard-deviation (1SD) of the last 2 minutes of each injected standard (N=18) is of 0.24 ± 0.02 ‰ and 0.47 ± 0.04‰ for $\delta^{18}O$ and δD, respectively.

3.3. Mixing induced by the instrumental CFA-system

We estimate the mixing length by means of isotopic liquid standards. In a first experiment, we applied an isotopic step at the MH with its concave volume filled (Fig.5, dataset MH-filled, N=4). The same step is then applied with the concave volume empty (Fig.5, dataset MH-empty, N=4). In addition to these two experiments, during each calibration procedure abrupt isotopic changes are realized at the water isotopes selection valve (Fig.5, dataset CRDS-line, N=15).

https://doi.org/10.5194/egusphere-2024-1807
Preprint. Discussion started: 15 July 2024

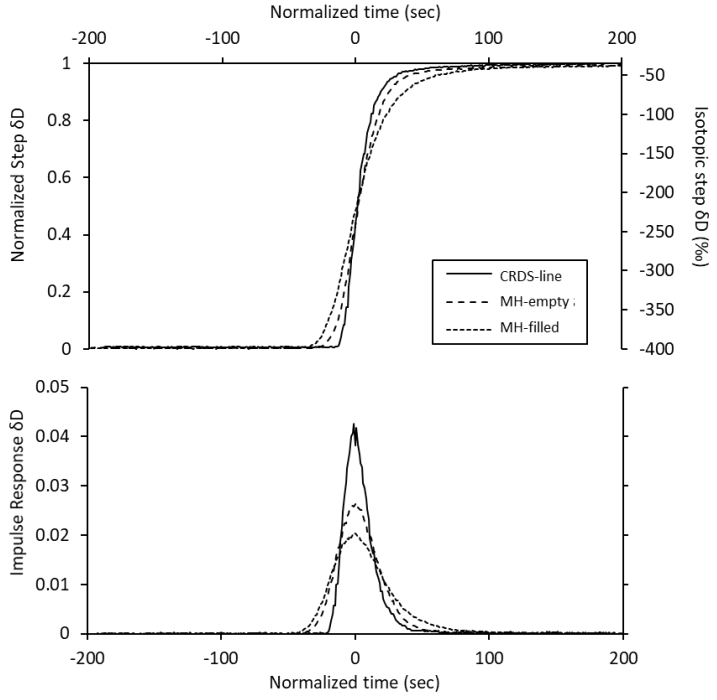

Figure 5: Isotopic step and impulse responses obtained for the three experiments realized. Isotopic switch at the isotope selection valve (WI-SV in Fig. 1) or at the Melt-Head (MH, Fig. 1), concave volume filled or empty.

Using equations (1) to (3), we compute the mixing lengths *(σ)* of our set of experiments ($\sigma_{MH\text{-}filled}$, $\sigma_{MH\text{-}empty}$, $\sigma_{CRDS\text{-}line}$). The results for both isotopologues δD and δ^{18}O are very similar, and we focus our study on the results for δD (Table 2). Furthermore, in addition to evaluating the mixing length induced by the whole CFA system, the combination of the three datasets allow us to distinguish between the contributions of the different parts of the system. Assuming independent mixings from each other from the Melt-Head to the CRDS instrument, the total mixing filter is the sum of the variances of each mixing filter along the CFA-system.

$$\sigma^2_{CFA-system} = \sigma^2_{MH-filled} = \sigma^2_{MH} + \sigma^2_{MH\ to\ WI-SV} + \sigma^2_{CRDS-line} \quad (6)$$

We can evaluate by quadrature difference (1) the mixing length induced by the concave volume of the MH ($\sigma_{MH} = \sqrt{\sigma^2_{MH-filled} - \sigma^2_{MH-empty}}$), as well as (2) the mixing length induced downstream of the MH to the isotopic selection valve ($\sigma_{MH\ to\ WI-SV} = \sqrt{\sigma^2_{MH-empty} - \sigma^2_{CRDS-line}}$).

https://doi.org/10.5194/egusphere-2024-1807
Preprint. Discussion started: 15 July 2024

$\sigma_{MH-filled}$	$\sigma_{MH-empty}$	$\sigma_{CRDS-line}$	σ_{MH}	$\sigma_{MH\ to\ WI-SV}$
21.6 (2.4)	*14.5 (1.2)*	*12.6 (1.8)*		
13.6 (1.5)	**9.2 (0.7)**	**8.0 (1.1)**	**10.0**	**4.5**

Table 2: δD means mixing length derived from the normal PDF, expressed in seconds (italic) and in mm (bold). Values in parenthesis represent 1SD. The conversion of seconds to mm is based on a melt-speed of 38 mm.min-1. σ_{MH} and $\sigma_{MH\ to\ WI-SV}$ correspond to differences in quadrature between $\sigma_{MH-filled}$ and $\sigma_{MH-empty}$, and between $\sigma_{MH-empty}$ and $\sigma_{CRDS-line}$, respectively.

We find a total mixing length of the AWI CFA system of ~14 mm (Table 2), indicating that the majority of the instrumental mixing is induced by the concave volume of the PICE design MH (10 mm mixing length), closely followed by the CRDS-line (8 mm). The tubular section in between, composed of tubes and the ~1ml safety volume of the debubbler, shows a significantly smaller contribution (4.5 mm).

3.4. Snow-core continuous records versus discrete records

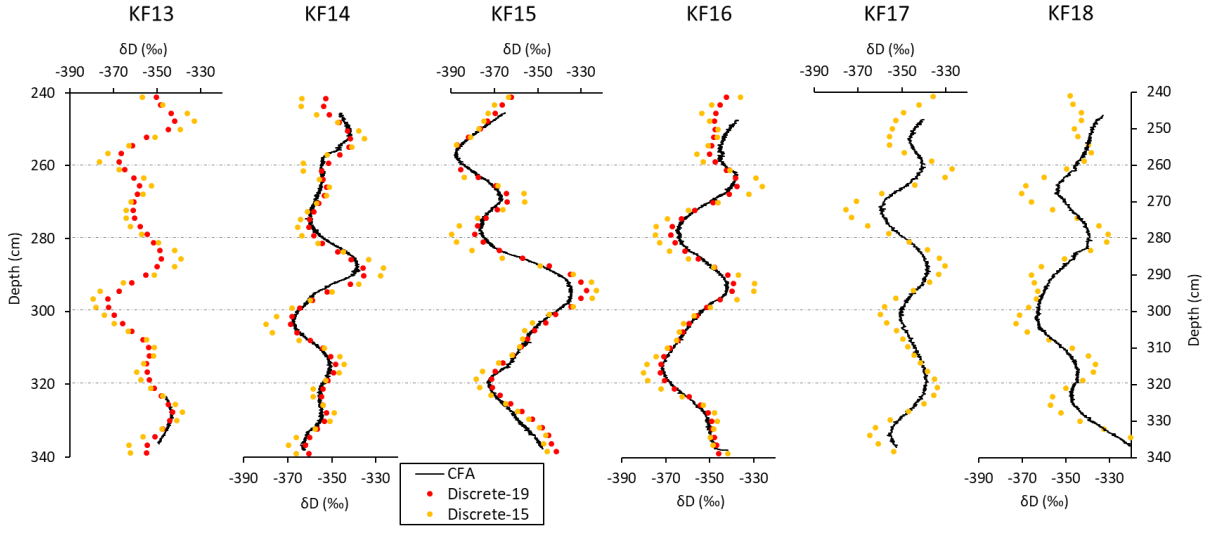

https://doi.org/10.5194/egusphere-2024-1807
Preprint. Discussion started: 15 July 2024

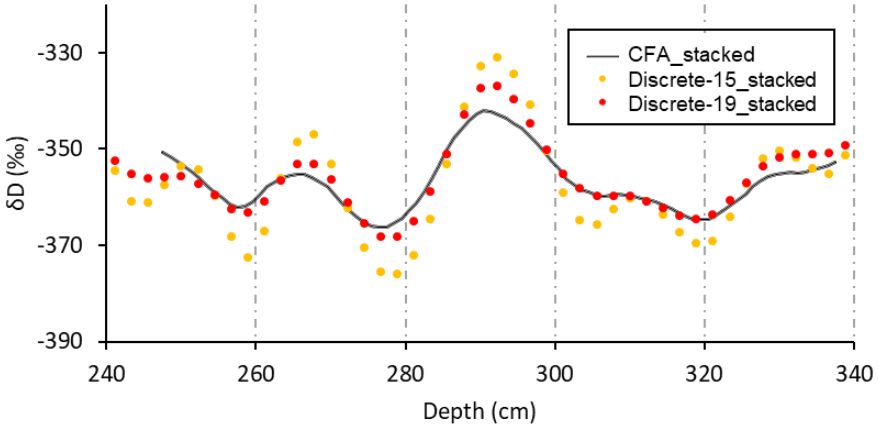

Figure 6: Top: 240-340 cm depth δD profiles of the six cores, 5 meters spaced. Datasets of continuous measurement (black lines), discrete-15 (orange markers) and discrete-19 (red markers) are shown. Because of the transition from MQ to sample and vice-versa, we removed the top-70 mm and bottom-20 mm of the continuous dataset. Note the small 150 mm portion of reliable continuous analysis for the core KF13, due to issues during the run. The averaged melt-speed of the 6 runs is 38 mm.min-1 (1SD = 9 mm.min-1). Bottom: Mean datasets of the stacked profiles KF-14, -15, -16.

We compare the discrete values from 2015 and 2019 as well as the values obtained from CFA at the single profiles (Fig. 6, upper panel) as well as at the mean profile, averaged over all profiles (Fig. 6 bottom) and quantify the differences. We first observe a mismatch in the depth assignment between discrete and CFA values – i.e., the phase of the records has an off-set of 12.3± 6.4 mm. The reason can be small-scale variations in density, leading to short-term changes in the melt-speed and thus affecting the depth-assignment of the CFA values. Secondly, comparing the amplitude between isotopic minima and maxima show that the continuous record attenuates on average ~17% of the discrete-19 record, and ~48% of the discrete-15 record. The strong difference between the two discrete datasets reveal a further and significant diffusional process occurring likely during the storage of the snow cores (Van der Wel et al., 2011).

Therefore, we use the discrete-19 dataset to assess the mixing of the CFA (section 3.4.1), and the discrete -15 dataset to investigate the effect of long-term storage on snow cores (section 3.4.2).

3.4.1 Mixing induced by continuous analysis of snow-core samples

When continuously analyzing a snow-core, due to the high-porosity of the upper-meters samples, capillary action (Colbeck, 1974) forces the melted water at the MH to lift upwards, enabling percolation (Fig. 7). Thus, by comparing the continuous dataset with a percolation-free discrete dataset, we aim to assess the mixing induced by the percolation.

https://doi.org/10.5194/egusphere-2024-1807
Preprint. Discussion started: 15 July 2024

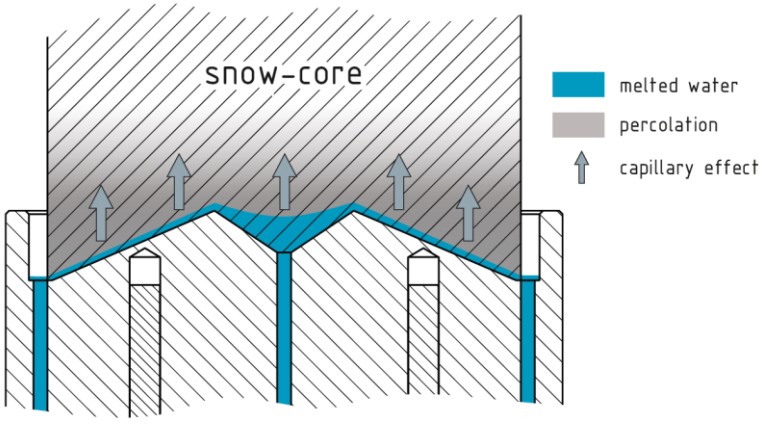

Figure 7: Illustration of the melting experiment showing the percolation induced by the low density of the sample combined to the melt-water reservoir within the inner concave volume of the MH.

In order to retrieve the mixing length induced by the continuous analysis of snow-cores with respect to the discrete dataset, we convolved the discrete signal with a family of impulse responses of different mixing lengths. A set of discrete-convolved signals of flattened extrema are obtained, and each signal is compared to the CFA signal (previously smoothed on 22 mm to ensure the same averaging than the discrete samples). Then, the minimum of root-mean-square (RMS = $\sqrt{mean\left(\left(x_i - x_j\right)^2\right)}$) between convolved signals and the continuous record allows for the identification of the adequate mixing length $\sigma_{CFA\text{-}discrete}$.

	KF13	KF14	KF15	KF16	KF17	KF18
$\sigma_{CFA-discrete19}$ Normal-CDF	x	29	32	31	x	x
$\sigma_{CFA-discrete15}$ Normal-CDF	x	49	52	57	56	57

Table 3: Mixing lengths (in mm) of the continuous profiles of δD, as related to the discrete-19 dataset and to the discrete-15 dataset. No results are available for the core KF13 due to the too short continuous dataset.

We find an average mixing length of approximately 30mm using the discrete 2019 dataset (Table 3). Following equation (6), we separate the mixing from the percolation at the MH from the remaining CFA system by:

$$\sigma^2_{CFA-discrete(i)} = \sigma^2_{CFA-system} + \sigma^2_{percolation} \quad (7)$$

$\sigma_{CFA\text{-}discrete(i)}$ refers to the overall mixing retrieved from the convolution of the discrete signal. $\sigma_{CFA\text{-}system}$ is the observed mixing of 14mm of the CFA system derived from experiments with the step function (section 3.3).

https://doi.org/10.5194/egusphere-2024-1807
Preprint. Discussion started: 15 July 2024

By retrieving the quadratic difference of CFA-discrete – CFA system we can compute the mixing length induced by the percolation at the MH with ~27 mm. This length is twice the length induced by the experimental system. Thus, percolation is the limiting factor on retrieved signal resolution when applying CFA on snow cores.

3.4.2. Smoothing of the isotope signal due to storage

We find a difference between the two discrete datasets 2015 and 2019 at the same snow cores, alongside with a mean $\sigma_{CFA\text{-}discrete15}$ value of ~54 mm (Table 3).

This difference is not related to instrumental induced mixing, but indicates the effect of long-term storage of snow samples. We assume, that the diffusion, taking place in snow and firn (Gkinis et al., 2014) is active in the cold store as well. Using our results, we can now quantity this storage-induced diffusion. Assuming that the mixing of the discrete-15 dataset corresponds to the mixing of the discrete-19 dataset convolved with an independent smoothing filter induced by the storage, comes:

$$\sigma^2_{CFA-discrete15} = \sigma^2_{CFA-discrete19} + \sigma^2_{storage\ 15-19} \quad (8)$$

Using the retrieved mixing lengths $\sigma_{CFA\text{-}discrete19}$ = 30 mm and $\sigma_{CFA\text{-}discrete15}$ = 54 mm, we derive a diffusion length of approximately 45 mm. These findings indicate, that during the 4 years of storage (first analysis in 2015 – versus second analysis in 2019) the isotope signal in the snow cores is smoothed by this diffusion length.

We further computed for each 1-meter long snow core the mean and variability (standard deviation) of the both discrete datasets (Table 4). The decrease in variability indicates an averaged attenuation of 0.54 ‰ and 4.5 ‰ for $\delta^{18}O$ and δD, respectively. The changes in the means show an averaged enrichment of isotopic composition of +0.31 ‰ for $\delta^{18}O$ and +1.6 ‰ for δD, likely due to the repeated contact with laboratory-air when bags are opened, and the loss of sample (frost) in the bag (personal communication, Sepp Kipfstuhl).

https://doi.org/10.5194/egusphere-2024-1807
Preprint. Discussion started: 15 July 2024

	$\delta^{18}O$ Discrete-15	$\delta^{18}O$ Discrete-19	δD Discrete-15	δD Discrete-19
KF13	-45.29 (1.3)	-45.076 (0.85)	-356.31 (11.93)	-355.77 (8.05)
KF14	-45.14 (1.45)	-44.71 (0.85)	-354.85 (12.24)	-353.12 (7.69)
KF15	-46.38 (2.39)	-45.91 (2.05)	-364.36 (19.53)	-361.51 (16.75)
KF16	-44.95 (1.70)	-44.76 (1.16)	-353.87 (14.72)	-353.30 (10.23)

Table 4: $\delta^{18}O$, δD means (standard deviation) for each snow core discrete dataset, expressed in ‰.

4. Discussion

With the newly developed CFA system for snow cores we measured in total 6 snow cores from the same location, retrieving a good agreement between the measurements. We find that a large portion of the smoothing of the isotope signal originates from the percolation at the inner concave volume of the PICE design MH. However, despite this limitation, the performances of our current experimental system with regards to the δD isotopic signal diffusion are similar to the improved CFA-CRDS system at University of Colorado (mixing length of 21.6 seconds, section 3.3 of this work, versus 19.1 seconds, Jones et al., 2017). Its application to low density cores (<400 kg.m^{-3}, Laepple et al., 2016) from low accumulation rate areas (Kohnen station, 200-300 mm recent annual gain of snow, Münch et al., 2017) gives relevant insights to the isotopic variations in spite of limitations in the measurements of their amplitudes.

To overcome the high-level of mixing induced by the percolation, it is crucial to prevent the formation of a reservoir of melt-water in contact with the snow-core, specifically in the inner volume at the MH. Thus, a new design of inner channel offers a possibility towards this aim. A flat surface covered with boreholes will allow for an efficient and uniform evacuation of the melt-water, limiting the suction upward. In addition to addressing the percolation, such design will significantly increase the experimental performances (section 3.3) in order to ultimately offer the necessary quality to resolve reliably the full isotopic cyclicity in the snowpack in low accumulation rate areas. Concerning very low accumulation rate sites, e.g. Vostock: ~60 mm annual snow layer thickness (Ekaykin et al., 2002); Dome F: ~74 mm (Kameda et al., 2008); Dome C: ~77 mm (Touzeau et al., 2016), additional improvements are necessary. The significant contribution of the CRDS-line (section 3.3) must here be addressed, and requires likely a collaboration with the manufacturer to improve the analytical unit itself (e.g. strong increase of volume at its inlet before a pressure-drop to the 40 Torr cavity).

The observation of the significant smoothing induced by the storage of the core samples is of particular interest. We show in Fig. B1 (Appendix B) the effect of storage on diffusion lengths for both isotopologues based on firn-diffusion model (Gkinis et al., 2014). Assuming a storage temperature of -20ºC and a low density of 370 kg.m^{-3}, 4 years lead to a very similar diffusion

https://doi.org/10.5194/egusphere-2024-1807
Preprint. Discussion started: 15 July 2024

length for δD than our quantification (section 3.4.3). The diffusivity coefficients being positively correlated to temperature (Fig. B2, Appendix B), the diffusion during storage is likely of stronger magnitude than on the East-Antarctic plateau.

5. Conclusions

Overcoming the increased stratigraphic noise in low accumulation areas and constraining the isotope signal formation within the upper-firn can be realized, but requires large number of high-quality stacked vertical profiles (Münch et al., 2017). In order to cope with the related challenge of high-pace -quality analysis and paired measurements of various proxies, we presented here a CFA-system adapted for analysis of snow-cores using the Niels-Bohr Institute design of Melt-Head (Kjaer et al. 2021). Based on standards and the method of Gkinis et al. (2011), we developed algorithms to quantify the smoothing of the isotopic signal induced by the system and inferred its major contributors. Using discrete samples, we further investigated and quantified the strong additional smoothing induced by the low density of the snow core samples. In order to offer a reliable high-resolution isotopic record in area of low accumulation rate such as Kohnen station, we recommend a new design of Melt-Head, with a focus on the evacuation of the melt-water. For very low accumulation rate sites however, using a CFA technique requires likely additional modification (i.e. mixing induced by the CRDS analytical device itself).

Finally, the isotopic diffusion during storage of snow-core samples requires further investigation, but underlines the need of (1) a strategy to preserve the original record (discrete samples cut in the field) or (2) prompt analysis with techniques such as the CFA.

https://doi.org/10.5194/egusphere-2024-1807
Preprint. Discussion started: 15 July 2024

APPENDIX A: CFA water isotope line

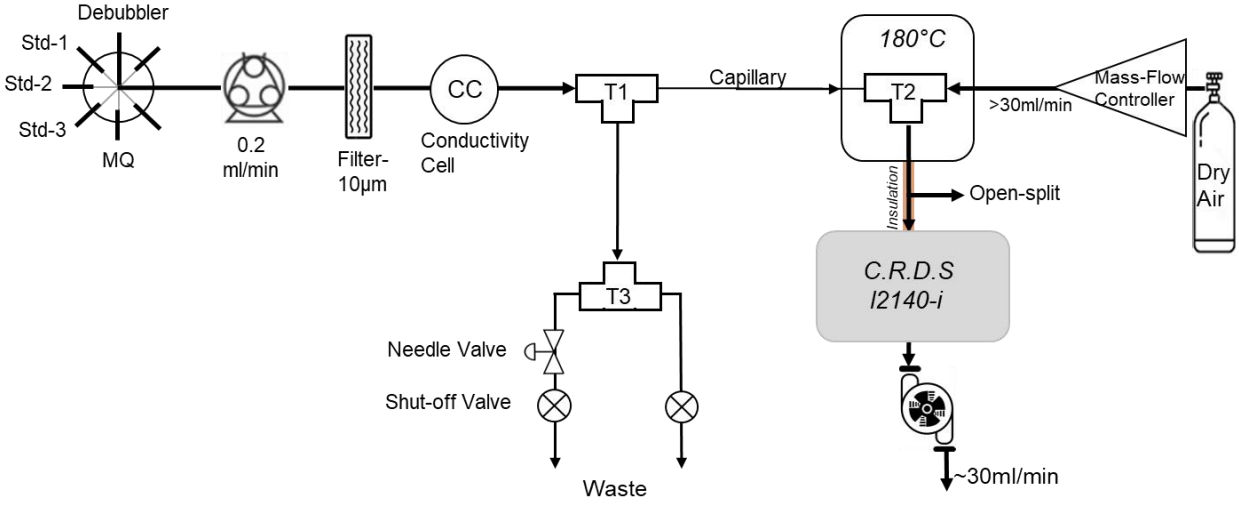

Figure A1: Detailed schematic of water isotopes line of the AWI CFA-system.

The selected sample steam is drained at a flow of ~0.2 ml.min^{-1} through PFA tubes of 0.51 mm ID to a 10 µm frits-filter (A-107, Idex), then a synchronization conductivity cell before entering a stainless-steel micro-volume tee (U-428, Idex; T1 in Fig. S1). Here, a micro-flow is split from the incoming stream into a fused-silica capillary tube (50 µm ID), the rest going into the waste line. Due to the smaller ID of the waste line (0.25 mm ID), a back-pressure pushes the micro-flow through the capillary towards the oven. To control this back-pressure precisely and efficiently, the waste line is divided using a PEEK tee (T3) and added to one of the two sub-waste lines a 10-turn micro-metering needle valve (P-445, Idex).

The sample micro-flow is injected into the stainless-steel tee (T2, Valco ZT1M) mounted in the 180°C oven, where it vaporizes instantly and mixes with a controlled flow of dry air (Mass Flow Controller SEC-E40 N2 100SCCM, Horiba company) to form a gas sample with the desired water vapor concentration.

https://doi.org/10.5194/egusphere-2024-1807
Preprint. Discussion started: 15 July 2024

APPENDIX B: Firn diffusion during storage

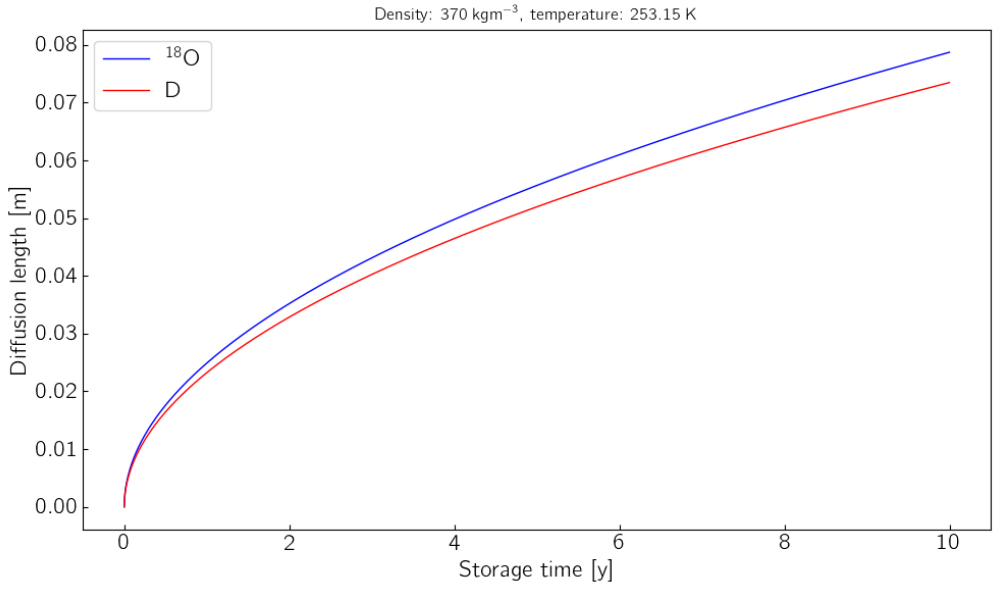

Figure B1: Firn-diffusion length for core samples (density of 370 kg.m^{-3}) as function of the time of storage (-20ºC).

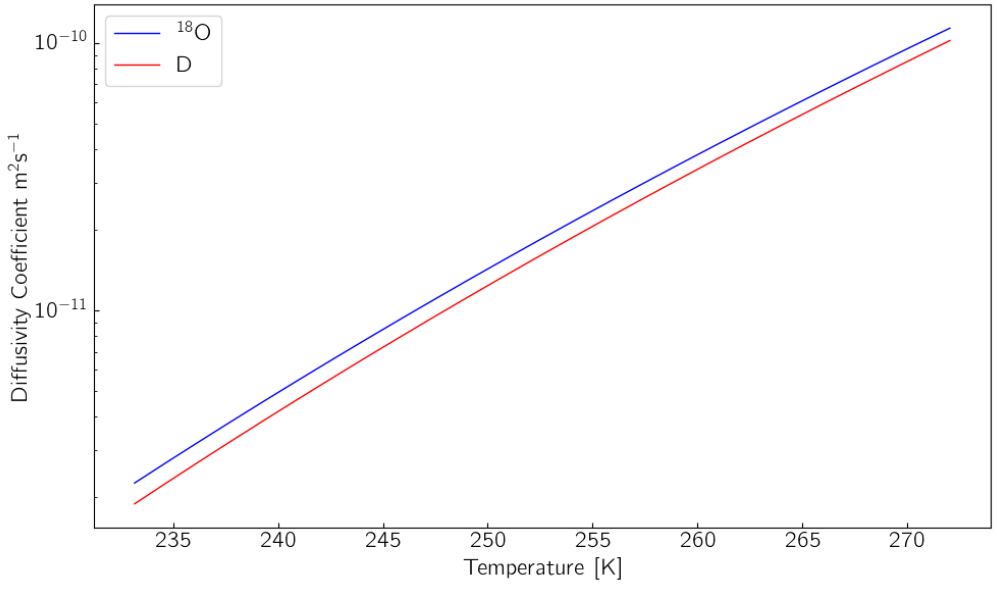

Figure B2: Diffusivity coefficients versus temperature.

https://doi.org/10.5194/egusphere-2024-1807
Preprint. Discussion started: 15 July 2024

Authors contribution

HM participated to the experiments, developed all the algorithms to characterize the isotopic diffusion using the R-software. VG provided his expertise on CFA and characterization of isotopic diffusion, and provided insights of the storage-effect based on firn-diffusion. Through the COMB-i project, MH and TL motivated the use of CFA with snow-cores. MB conducted all discrete isotopic measurements at AWI-Bremerhaven. RD developed the CFA-system, designed and proceeded to the tests, experiments, analysis, and co-supervised the diffusion characterization Master-thesis. All authors contributed to the writing of the manuscript.

Competing interests

The authors declare that they have no conflict of interest.

Data availability

The algorithms developed in R to characterize the isotopic diffusion are available at: https://github.com/Ice-core-Paleo-Proxies/AWI_CFA_Isotope. The snow-cores discrete samples isotopic datasets 2015 and 2019 are archived at the PANGAEA database, under https://doi.pangaea.de/10.1594/PANGAEA.939208 and https://doi.pangaea.de/10.1594/PANGAEA.939207, respectively.

The snow-cores continuous high-resolution profiles are archived under https://doi.pangaea.de/10.1594/PANGAEA.939181.

PANGAEA is hosted by the Alfred Wegener Institute Helmholtz Centre for Polar and Marine Research (AWI), Bremerhaven, and the Center for Marine Environmental Sciences (MARUM), Bremen, Germany.

Acknowledgmnent

This project was supported by Helmholtz funding through the Polar Regions and Coasts in the Changing Earth System (PACES) programme of the Alfred Wegener Institute. RD is currently financed by the PAIGE (Chronologies for Polar Paleoclimate Archives – Italian-German Partnership) project, and TL was supported by the European Research Council (ERC) under the European Union's Horizon 2020 Research and Innovation Programme (grant agreement no. 716092). We are grateful to Helle-Astrid Kjaer and Paul Vallelonga for providing the design of Melt-Head for snow-cores, and the AWI-Workshop for manufacturing. We thank Thaddäus Bluszcz for his help at the first stage of the instrumental development, and York Schlomann for providing all necessary isotopic standards. We further thank Hanno Meyer for the discrete-15 isotopic measurement and Thomas Münch for providing all information for the snow-cores investigation. Finally, the main author is very grateful to Johannes Freitag and Sepp Kipfstuhl for their relevant inputs on the data analysis.

https://doi.org/10.5194/egusphere-2024-1807
Preprint. Discussion started: 15 July 2024

References

Allan, D. W.: Statistics of atomic frequency standards, P. IEEE, 54, 221–230, 1966.

Bigler, M.; Svensson, A.; Kettner, E.; Vallelonga, P.; Nielsen, M.E.; Steffensen, J. P. Optimization of High-Resolution Continuous Flow Analysis for Transient Climate Signals in Ice Cores. Environ. Sci.Technol. 2011, 45, 4483−4489.

Breton, D.J., Koffman, B.G., Kurbatov, A.V., Kreutz, K.J. and Hamilton, G.S. (2012): Quantifying Signal Dispersion in a Hybrid Ice Core Melting System. Environ. Sci. Technol., 46(21), 11922-11928, doi: 10.1021/es302041k.

Colbeck, S. (1974). The capillary effects on water percolation in homogeneous snow. Journal of Glaciology, 13(67), 85-97. doi:10.3189/S002214300002339X

Dallmayr, R., Goto-Azuma, K., Kjær, H. A., Azuma, N., Takata, M., Schüpbach, S. and Hirabayashi, M.: A High-Resolution Continuous Flow Analysis System for Polar Ice Cores, Bull. Glaciol. Res., 34, 11–20, https://doi.org/10.5331/bgr.16R03, 2016.

Drücker, C., Wilhelms, F., Oerter, H., Frenzel, A., Gernandt, H. and Miller, H. (2002): Design, transport, construction, and operation of the summer base Kohnen for ice-core drilling in Dronning Maud Land, Antarctica., Ice drilling technology 2000: Proceedings of the fifth International Workshop on Ice Drilling Technology, 30 October-1 November 2000, Nagaoka University of Technology, Nagaoka, pp. 302-312.

Ekaykin, A. A., Lipenkov, V. Y., Barkov, N. I., Petit, J. R., and Masson-Delmotte, V.: Spatial and temporal variability in isotope composition of recent snow in the vicinity of Vostok station, Antarctica: implications for ice-core record interpretation, Ann. Glaciol., 35, 181–186, doi:10.3189/172756402781816726, 2002.

Fisher, D. A., Reeh, N., and Clausen, H. B.: Stratigraphic noise in time series derived from ice cores, Ann. Glaciol., 7, 76–83, doi:10.3198/1985AoG7-1-76-83, 1985.

Gkinis, V., Popp, T. J., Johnsen, S. J., and Blunier, T.: A continuous stream flash evaporator for the calibration of an IR cavity ring down spectrometer for isotopic analysis of water, Isot. Environ. Health S., 46, 1–13, 2010.

Gkinis, V., Popp, T. J., Blunier, T., Bigler, M., Schüpbach, S., Kettner, E., and Johnsen, S. J.: Water isotopic ratios from a continuously melted ice core sample, Atmos. Meas. Tech., 4, 2531–2542, doi:10.5194/amt-4-2531-2011, 2011.

Gkinis V., Simonsen S. B., Buchardt S. L., White J. W. C. and Vinther B. M. (2014) Water isotope diffusion rates from the NorthGRIP ice core for the last 16,000 years – glaciological and paleoclimatic implications. Earth Planet. Sci. Lett., 405.

Göktas, F., Fischer, H., Oerter, H., Weller, R., Sommer, S., & Miller, H. (2002). A glacio-chemical characterization of the new EPICA deep-drilling site on Amundsenisen, Dronning Maud Land, Antarctica. Annals of Glaciology, 35, 347-354. doi:10.3189/172756402781816474

Hoshina, Y., K. Fujita, F. Nakazawa, Y. Iizuka, T. Miyake, M. Hirabayashi, T. Kuramoto, S. Fujita, and H. Motoyama (2014), Effect of accumulation rate on water stable isotopes of near-surface snow in inland Antarctica, J. Geophys. Res. Atmos., 119, 274–283, doi:10.1002/2013JD020771.

https://doi.org/10.5194/egusphere-2024-1807
Preprint. Discussion started: 15 July 2024

Jones, T.R.; White, James W C; Steig, Eric J.; Vaughn, Bruce H.; Morris, Valerie; Gkinis, Vasileios; Markle, Bradley R.; Schoenemann, Spruce W. (2017), "Improved methodologies for continuous-flow analysis of stable water isotopes in ice cores", Atmos. Meas. Tech., 10, 617–632, doi.org/10.5194/amt-10-617-2017.

Jouzel J., Alley, R. B., Cuffey, K. M., Dansgaard, W., Grootes, P., Hoffmann, G., Johnsen, S. J., Koster, R. D., Peel, D., Shuman, C. A., Stievenard, M., Stuiver, M., White, J. (1997). Validity of the temperature reconstruction from water isotopes in ice cores. Journal of Geophysical Research 102(C12), 471–487 doi: 10.1029/97JC01283.

Kameda, T., Motoyama, H., Fujita, S., and Takahashi, S.: Temporal and spatial variability of surface mass balance at Dome Fuji, East Antarctica, by the stake method from 1995 to 2006, J. Glaciol., 54, 107–116, doi:10.3189/002214308784409062, 2008.

Kawamura, K., A. Abe-Ouchi, H. Motoyama, Y. Ageta, S. Aoki, N. Azuma, Y. Fujii, K. Fujita, S. Fujita, and K. Fukui (2017), State 30 dependence of climatic instability over the past 720,000 years from Antarctic ice cores and climate modeling, Science advances, 3(2), e1600,446.

Kjaer et al., 2021, A portable Lightweight In Situ Analysis (LISA) box for ice and snow analysis, The Cryosphere, 15, 3719–3730, 2021 https://doi.org/10.5194/tc-15-3719-2021

Laepple, T., Hörhold, M., Münch, T., Freitag, J., Wegner, A., and Kipfstuhl, S.: Layering of surface snow and firn at Kohnen Station, Antarctica: Noise or seasonal signal? J. Geophys. Res. Earth Surf., 121, 1849–1860, doi:10.1002/2016JF003919, 2016.

Laepple, T., Münch, T., Casado, M., Hoerhold, M., Landais, A., and Kipfstuhl, S.: On the similarity and apparent cycles of isotopic variations in East Antarctic snow pits, The Cryosphere, 12, 169–187, https://doi.org/10.5194/tc-12-169-2018, 2018

Maselli, O. J., Fritzsche, D., Layman, L., McConnell, J. R. & Meyer, H. Comparison of water isotope-ratio determinations using two cavity ring-down instruments and classical mass spectrometry in continuous ice-core analysis. Isotopes Environ. Health Stud. 387–398, https://doi.org/10.1080/10256016.2013.781598 (2013)

Moser, D.E., Hoerhold, M., Kipfstuhl, S., Freitag, J. (2020) Microstructure of Snow and Its Link to Trace Elements and Isotopic Composition at Kohnen Station, Dronning Maud Land, Antarctica. Front. Earth Sci. 8:23. doi: 10.3389/feart.2020.00023

Münch, T., Kipfstuhl, S., Freitag, J., Meyer, H., and Laepple, T.: Regional climate signal vs. local noise: a twodimensional view of water isotopes in Antarctic firn at Kohnen Station, Dronning Maud Land, Clim. Past, 12, 1565–1581, https://doi.org/10.5194/cp-12-1565-2016, 2016

Münch, T., Kipfstuhl, S., Freitag, J., Meyer, H., and Laepple, T.: Constraints on post-depositional isotope modifications in East Antarctic firn from analysing temporal changes of isotope profiles, The Cryosphere Discuss., 2017, 1–21, doi:10.5194/tc-2017-35, 2017

Münch, T. and Laepple, T. (2018). What climate signal is contained in decadal- to centennial-scale isotope variations from Antarctic ice cores? Climate of the Past, 14, 2053–2070, doi: 10.5194/cp-14-2053-2018

Oerter, H., Drücker, C., Kipfstuhl, S., Wilhelms, F. (2009): Kohnen Station - the Drilling Camp for the EPICA Deep Ice Core in Dronning Maud Land, Polarforschung; 78, 1-2; 1-23

https://doi.org/10.5194/egusphere-2024-1807
Preprint. Discussion started: 15 July 2024

Osterberg, E.C., Handley, M.J., Sneed, S.B., Mayewski, P.A. and Kreutz, K.J. (2006): Continuous Ice Core Melter System with Discrete Sampling for Major Ion, Trace Element, and Stable Isotope Analyses. Environ. Sci. Technol., 40(10), 3355-3361, doi: 10.1021/es052536w

Petit, R. J., D. Raynaud, I. Basile, J. Chappellaz, C. Ritz, M. Delmotte, M. Legrand, C. Lorius, L. Pe, J. R. Petit, J. Jouzel, D. Raynaud, N. I. Barkov, J. M. Barnola, I. Basile, M. Bender, J. Chappellaz, M. Davis, G. Delaygue, M. Delmotte, V. M. Kotlyakov, M. Legrand, V. Y. Lipenkov, C. Lorius, L. Pepin, C. Ritz, E. Saltzman, and M. Stievenard (1999), Climate and atmospheric history of the past 420,000 years from the Vostok ice core, Antarctica, Nature, 399(6735), 429–436

Ruth, U., D. Wagenbach, M. Bigler, J. P. Steffensen, and R. Röthlisberger, High resolution dust profiles at NGRIP: Case studies of the calcium-dust relationship, Ann. Glaciol., 35, 2002.

Schaller, C. F., Freitag, J., Kipfstuhl, S., Laepple, T., Steen-Larsen, H. C., and Eisen, O.: A representative density profile of the North Greenland snowpack, The Cryosphere, 10, 1991–2002, https://doi.org/10.5194/tc-10-1991-2016, 2016.

Steinhage, D., Kipfstuhl, S., Nixdorf, U., & Miller, H. (2013). Internal structure of the ice sheet between Kohnen station and Dome Fuji, Antarctica, revealed by airborne radio-echo sounding. Annals of Glaciology, 54(64), 163-167. doi:10.3189/2013AoG64A113

Touzeau, A., Landais, A., Stenni, B., Uemura, R., Fukui, K., Fujita, S., Guilbaud, S., Ekaykin, A., Casado, M., Barkan, E., Luz, B., Magand, 20 O., Teste, G., Le Meur, E., Baroni, M., Savarino, J., Bourgeois, I., and Risi, C.: Acquisition of isotopic composition for surface snow in East Antarctica and the links to climatic parameters, The Cryosphere, 10, 837–852, doi:10.5194/tc-10-837-2016, 2016.

Van der Wel, L., Gkinis, V., Pohjola, V., & Meijer, H. (2011). Snow isotope diffusion rates measured in a laboratory experiment. Journal of Glaciology, 57(201), 30-38. doi:10.3189/002214311795306727